# Analyses of the complete genome sequence of 2,6-dichlorobenzamide (BAM) degrader *Aminobacter* sp. MSH1 suggests a polyploid chromosome, phylogenetic reassignment, and functions of (un)stable plasmids.

**Running title: Complete genome of *Aminobacter* sp. MSH1**

## Authors

Tue Kjærgaard Nielsen[a†], Benjamin Horemans[b†], Cedric Lood[c,d], Jeroen T'Syen[e], Vera van Noort[c], Rob Lavigne[d], Lea Ellegaard-Jensen[f], Ole Hylling[f], Jens Aamand[g], Dirk Springael[e‡*], Lars Hestbjerg Hansen[a‡*]

[†]These authors contributed equally to the work presented

[‡] DS and LHH initiated the study and supervised the project equally in separate labs

## Institutional Affiliation

[a] University of Copenhagen, Faculty of Science, Department of Plant and Environmental Sciences, Section for Microbiology and Biotechnology, Copenhagen, Denmark

[b] BAT Knowledge Centre, Sustainable Materials Unit, Vlaams Instituut voor Technologisch Onderzoek, Mol, Belgium

[c] KU Leuven, Faculty of Bioscience Engineering, Department of Microbial and Molecular Systems (M²S), Centre of Microbial and Plant Genetics, Leuven, Belgium

[d] KU Leuven, Faculty of Bioscience Engineering, Department of Biosystems, Laboratory of Gene Technology, Leuven, Belgium

[e] KU Leuven, Faculty of Bioscience Engineering, Department of Earth and Environmental Sciences, Division of Soil and Water Management, Leuven, Belgium

[f] Aarhus University, Department of Environmental Science, Section of Environmental Microbiology and Circular Resource Flow, Roskilde, Denmark

[g] Geological Survey of Denmark & Greenland (GEUS), Department of Geochemistry, Copenhagen, Denmark

## Corresponding authors

* Professor Dirk Springael

KU Leuven

Faculty of Bioscience Engineering

Department of Earth and Environmental Sciences

Division of Soil and Water Management

Kasteelpark Arenberg 20 bus 2459

3001 Leuven

Phone: +32 16321604

E-mail: dirk.springael@kuleuven.be

and

* Professor Lars H. Hansen

Microbial Ecology and Biotechnology

Department of Plant and Environmental Sciences

University of Copenhagen

Thorvaldsensvej 40

1871 Frederiksberg, Denmark

Mobile: +45 28752053

E-mail: lhha@plen.ku.dk

## Abstract

*Aminobacter* sp. MSH1 (CIP 110285) can use the pesticide dichlobenil and its transformation product, the recalcitrant groundwater micropollutant, 2,6-dichlorobenzamide (BAM) as sole source of carbon, nitrogen, and energy. The concentration of BAM in groundwater often exceeds the threshold limit for drinking water, resulting in the use of additional treatment in drinking water treatment plants (DWTPs) or closure of the affected abstraction wells. Biological treatment with MSH1 is considered a potential sustainable alternative to remediate BAM-contamination in drinking water production. Combining Illumina and Nanopore sequencing, we here present the complete genome of MSH1, which was determined independently in two different laboratories. Unexpectedly, divergences were observed between the two genomes, i.e. one of them lacked four plasmids compared to the other. Besides the circular chromosome and the two previously described plasmids involved in BAM catabolism pBAM1 (41 kb) and pBAM2 (54 kb), we observe that the genome of MSH1 contains two megaplasmids pUSP1 (367 kb) and pUSP2 (366 kb) and three smaller plasmids pUSP3 (97 kb), pUSP4 (64 kb), and pUSP5 (32 kb). The MSH1 substrain from KU Leuven showed a reduced genome lacking plasmids pUSP2 and the three smaller

plasmids and was designated substrain MK1, whereas the variant with all plasmids was designated as substrain DK1. Results of a plasmid stability experiment, indicate that strain MSH1 may have a polyploid chromosome when growing in R2B medium with more chromosomes than plasmids per cell. Based on phylogenetic analyses, strain MSH1 is reassigned as *Aminobacter niigataensis* MSH1.

## Importance

The complete genomes of the two MSH1 substrains, DK1 and MK1, provide further insight into this already well-studied organism with bioremediation potential. The varying plasmid contents in the two substrains suggest that some of the plasmids are unstable, although this is not supported by the herein described plasmid stability experiment. Instead, results suggest that MSH1 is polyploid with respect to its chromosome, at least under some growth conditions. As the essential BAM-degradation genes are found on some of these plasmids, stable inheritance is essential for continuous removal of BAM. Finally, *Aminobacter* sp. MSH1 is reassigned as *Aminobacter niigataensis* MSH1, based on phylogenetic evidence.

## Keywords

*Aminobacter*, 2,6-dichlorobenzamide, *Phyllobacteriaceae*, Nanopore sequencing, catabolic plasmids

## Introduction

The occurrence of organic micropollutants in different water compartments threatens both ecosystem functioning as well as future drinking water supplies (1). Organic micropollutants are

organic chemicals with complex and highly variable structures, and they have in common that they occur in the environment at trace concentrations (in the µg – ng/L range). Organic micropollutants often have unknown ecotoxicological and/or human health effects. They include a multitude of compounds such as pharmaceuticals, pesticides, ingredients of household products and additives of personal care products. In the European Union, the threshold limit for pesticides and relevant transformation products in drinking water is set at 0.1 µg/L (2). This threshold is frequently exceeded and forces drinking water treatment plants to invest in expensive physicochemical treatment technologies or to close groundwater extraction wells (3). The use of pollutant degrading bacteria in bioaugmentation strategies to remove micropollutants, such as pesticides, from drinking water, is presented as a solution (3,4). The groundwater micropollutant 2,6-dichlorobenzamide (BAM), a transformation product of the herbicide dichlobenil, frequently occurs in groundwater in Europe, often exceeding the treshold concentration (5). *Aminobacter* sp. MSH1 (CIP 110285) was enriched and isolated from dichlobenil treated soil sampled from the courtyard of a plant nursery in Denmark. The strain converts dichlobenil to BAM, which is further fully mineralized (6). Efforts to elucidate the catabolic pathway for BAM degradation in MSH1 revealed the involvement of two plasmids. The first step of BAM-mineralization involves the hydrolysis of BAM to 2,6-dichlorobenzoic acid (2,6-DCBA) by the amidase BbdA encoded on the 41 kb IncP1-β plasmid pBAM1 (7). Further catabolism of 2,6-DCBA to central metabolism intermediates involves enzymes encoded on the 54 kb *repABC* family plasmid pBAM2. The strain mineralizes BAM at trace concentrations (6) and invades biofilms of microbial communities of rapid sand filters used in DWTPs (8). Moreover, it was successfully used in bioaugmentation of rapid sand filters, both in lab scale and pilot scale biofilration systems, to remove BAM from (ground)water (8–11). On the other hand, long-term population persistence and catabolic activity in the sand

filters were impeded, likely due to a combination of predation and wash out (11, 12), as well as to physiological and genetic changes. Reducing flow rate and improving inoculation strategy have demonstrated prolonged persistence and activity of MSH1 in bioaugmented sand filters (13). However, other studies indicate that MSH1 shows a starvation survival response, in the nutrient (especially carbon) limiting environment of DWTPs, leading to reduced specific BAM degrading activity (14). Moreover, a substantial loss of plasmid pBAM2 was observed upon prolonged transfer of MSH1 both in R2A medium and in C-limited minimal medium (15), indicating that the plasmid is not entirely stable. Moreover, mutants lacking the ability to convert BAM into 2,6-DCBA have been reported (7). Clearly, to come to full management of bioaugmentation using MSH1 in DWTP biofiltration units aiming at BAM removal, more knowledge is needed on the physiological as well as genetic adaptations of MSH1 when introduced into the corresponding oligotrophic environment. The elucidation of the full genome sequence is crucial in this.

The complete genome sequence presented in this study shows that MSH1 substrain DK1 has a single chromosome and seven plasmids, including the two previously described catabolic plasmids pBAM1 and pBAM2, while substrain MK1 lacks four of these plasmids. The relative sequence coverage of the plasmids compared to the chromosome suggested that there are either multiple copies of the chromosome per cell or that there are, on average, fewer than one copy of six out of the seven plasmids per cell. This was tested in a plasmid stability experiment with substrain DK1 where plasmids were found to be overall stable, with the exception of a single loss event of pUSP1. This supports the hypothesis that MSH1 might have a polyploid chromosome, at least under some growth conditions.

# Material and Methods

*Growth conditions, genomic DNA preparation and sequencing*

The genome sequence of strain MSH1 was independently obtained in two different laboratories, i.e., the KU Leuven in Belgium (MK1) and the Aarhus University lab in Roskilde, Denmark (DK1). In both cases, *Aminobacter* sp. MSH1 was obtained from the strain collection of the laboratory that originally isolated the bacterium (6). Sequencing of substrain DK1 at the Roskilde lab was performed as follows. Directly derived from a cryostock obtained from the original lab of MSH1, two ml of a culture grown in R2B were used for extraction of high molecular weight (HMW) DNA using the MasterPure™ DNA Purification Kit (Epicentre, Madison, WI, USA), using the kit's protocol for cell samples. DNA was eluted in 35 µL 10 mM Tris-HCl (pH 7.5) with 50 mM NaCl. The purity and concentration of extracted DNA were measured with a NanoDrop 2000c and a Qubit® 2.0 fluorometer (Thermo Fisher Scientific, Walther, MA, USA), respectively. An Illumina Nextera XT library was prepared for paired-end sequencing on an Illumina NextSeq 500 with a Mid Output v2 kit (300 cycles) (Illumina Inc., San Diego, CA, USA). Paired-end reads (2x151 bp) were trimmed for contaminating adapter sequences and low quality bases (<Q20) at the ends of the reads were removed using Cutadapt (v1.8.3) (16). Paired-end reads that overlapped were merged with AdapterRemoval (v2.1.0) (17). For Oxford Nanopore sequencing, a library was prepared from the same DNA extract using the Rapid Sequencing kit (SQK-RAD004). This was loaded on an R9.4 flow cell and sequenced using MinKnow (v1.11.5) (Oxford Nanopore Technologies, Oxford, UK). Nanopore reads were basecalled with albacore (v2.1.10) without quality filtering of reads. Only reads longer than 5,000 bp were retained and sequencing adapters were trimmed using Porechop (v0.2.3). A hybrid genome assembly with Nanopore and Illumina reads was performed using Unicycler (v0.4.3) (18).

147 The Illumina sequencing of substrain MK1 in the KU Leuven lab was reported previously (7, 19).
148 Briefly, genomic DNA was isolated from a culture grown on R2B using the Puregene Core kit A
149 (Qiagen, Hilden, Germany), according to the manufacturer's instructions, except that DNA
150 precipitation was performed with ethanol. A library was constructed for paired-end sequencing
151 using 500 bp inserts and sequencing was performed on the Illumina GAIIx platform. Generated
152 read lengths were 90 bp. The Illumina reads were quality controlled using FastQC (20) (v0.11.6)
153 and BBduk (21) (v36.47). This included trimming the reads with low scoring regions (Phred < 30),
154 clipping adapters, and removing very short reads (length < 50). For Nanopore sequencing, total
155 genomic DNA was extracted from a culture grown on R2B with 200 mg/L BAM using the DNeasy
156 UltraClean Microbial Kit (Qiagen, Hilden, Germany ). Afterwards, the genomic DNA was
157 mechanically sheared using a Covaris g-Tube (Covaris Inc., MA, USA) to an average fragment
158 length of 8 kb. The library for sequencing was prepared using the 1D ligation approach with native
159 1D barcoding (SQK-LSK109) and sequenced on a MinION R9.4 flow cell using the MinION
160 sequencer (Oxford Nanopore Technologies, Oxford, UK). The Nanopore reads were basecalled
161 with Albacore (v2.0.2), and the barcode sequences were trimmed using Porechop (v0.2.3). Hybrid
162 assembly of genome was performed as reported above.

163 *Genome analyses*

164 For both genomes, automatic gene annotation was done using Prokka (22) (v1.14.0). Separately
165 from Prokka, proteins with transmembrane helices were identified using TMHMM v2.0 (23).
166 Genes were assigned to COG functional categories using EggNOG-mapper v4.5.1 (24). Genome
167 comparison was done using EDGAR (25). Metabolic pathways were explored using Pathway
168 Tools (26) and RAST (27). Circularized views of chromosome and plasmids were made using
169 Circos (28). MegaX (29) was used for protein alignment and tree building. Phylogenetic analysis

for strain MSH1 was performed using a clustal-omega (30) multiple sequence alignment using 16S ribosomal RNA genes from the set of type strains available in the *Phyllobacteriaceae* family. The tree was inferred using PhyML (31) with a GTR substitution model and a calculation of branch support values (bootstrap value of 1,000). Whole-genome-based taxonomic classification was performed with *in silico* DNA:DNA hybridization using the Type Strain Genome Server (TYGS) (32). Furthermore, average nucleotide identity (ANI) values were calculated for MSH1 against all available *Aminobacter* genomes in NCBI (downloaded January 31, 2021), using FastANI (33) and plotted in R with the *pheatmap* package (34). Genomes of the two MSH1 substrains were compared using the Mauve genome alignment software (35). Plasmids were characterized with regards to relaxase genes and replicon families using MOB-suite (36).

*Plasmid (in)stability experiment*

To test for plasmid stability, MSH1 cells from -80°C cryostock were streaked on R2A plates and DNA from 1 ml of the cryostock was extracted using MasterPure™ DNA Purification Kit. After incubation at 22°C for 11 days, a single colony from the R2A plate was picked and resuspended in 105 µl phosphate-buffered saline (PBS). From this, 5 µl suspension was inoculated in 25 ml R2B for 72 hours. Whole genome sequencing was performed on the remaining 100 µl PBS suspension. After 72 hours of growth in R2B, 1 mL broth culture was sampled for DNA extraction, similarly to the DNA extracted for initial DNA sequencing (above), and 100 µL of dilution series $10^{-5}$-$10^{-8}$ of the R2B culture were plated onto R2A and the plates incubated at 22°C. After 7 days of growth, DNA was extracted and sequenced, as described above, from 14 individual colonies (originating from a single cell) resuspended in 100 µL PBS. All sequencing was performed on an

Illumina NextSeq 550 with a Mid Output v2 kit (300 cycles) using Nextera XT library preparations as described above.

Sequencing adapters and poor quality sequences were trimmed from paired end reads using Trimmomatic (v0.39) (37) with the options "ILLUMINACLIP:/usr/share/trimmomatic/NexteraPE-PE.fa:2:30:10 LEADING:3 TRAILING:3 SLIDINGWINDOW:4:15 MINLEN:36". Trimmed and filtered reads from each replicate MSH1 sample were mapped with bwa (v0.7.17-r1198-dirty) (38) to the completely assembled MSH1 genome including plasmids pBAM1-2 and pUSP1-5. Sequencing coverage in 1,000 bp windows for all replicons per replicate sample was calculated with samtools (v1.9-166-g74718c2) (39) and bedtools (v2.28.0) (40). Coverage data for all replicons were divided by the mean coverage of the chromosome, in order to normalize replicon copy numbers relative to the chromosome. Normalized coverage of all replicons for all replicates were visualized with Circos (v0.69-6) (28).

*Data availability*

The genome sequences of strain MSH1 substrains MK1/DK1 are available under the following GenBank accession numbers CP026265/CP028968 (chromosome), CP026268/CP028967 (pBAM1), CP026267/CP028966 (pBAM2), CP026266/CP028969 (pUSP1) and CP028970 (pUSP2), CP028971 (pUSP3), CP028972 (pUSP4) and CP028973 (pUSP5).

## Results and discussion

*Genome statistics*

The MSH1 genome (based on substrain DK1) consists of a chromosome of 5,301,518 bp and seven plasmids. The genome contains two large plasmids pUSP1 of 367,423 bp and pUSP2 of 365,485

bp, three smaller plasmids pUSP3, pUSP4, and pUSP5 (respectively 97,029 bp, 64,122 bp, and 31,577 bp) and the two previously reported smaller catabolic plasmids pBAM1 and pBAM2 of 40,559 bp and 53,893 bp, respectively (Table 1). A total of 6,257 genes could be predicted of which six rRNAs, 53 tRNAs, and four ncRNAs. A total of 6,194 CDS were predicted including 190 pseudogenes (Table 2). Circular views of the chromosome and seven plasmids are shown in Figure 1 and 2. The KU Leuven variant, designated as substrain MK1, lacked one of the two larger plasmids, i.e. pUSP2, and the three smaller plasmids pUSP3, pUSP4, and pUSP5. Except for the discrepancy in plasmids, the shared genomes (chromosome, pUSP1, pBAM1, and pBAM2) of the two strains have an average nucleotide identity of 99.9925%. The BAM-catabolic genes were manually checked for mutations that could indicate differences in degradation potential. A single nucleotide change was noted in the *bbdb3* gene on pBAM2, encoding one of three subunits of a TRAP-type transport system potentially involved in the uptake of 2,6-DCBA (19). In this gene, a non-synonomous substitution has changed a glycine to an arginine in the resulting protein in MK1. Currently, it is not known if this change has an effect on the putative function of this tripartite transport system. Furthermore, differences were found in the region of plasmid pUSP1 containing an IS*30* family insertion sequence with 38 bp flanking, imperfect, inverted repeats (IRs). The repeats appear complete in DK1, but MK1 shows a deletion of 56 bp and 34 bp up- and downstream of the IS*30* transposase gene, including partial deletion of the IR at both ends, suggesting that the MK1 substrain has undergone further genetic changes. The deletions flanking the IS*30* element on pUSP1 in MK1 may have been caused by a possible intramolecular transposition event (41). However, this IS*30* element with deletion in the IRs in MK1 may still be functional, as the functional core region of IS*30* IRs are only part of the complete IR (42).

236

237 *Phylogenetic assignment of MSH1 to* Aminobacter niigataensis

238 A phylogenetic tree based on the 16S rRNA gene sequence indicating the position of MSH1 is
239 shown in Figure 3. The 1,463 bp 16S rRNA gene sequence of MSH1 is 100% identical to that of
240 *Aminobacter niigataensis* DSM 7050$^{T}$ and 99.6-99.8% to those of other *Aminobacter* species. This
241 is supported by whole-genome *in silico* digital DNA:DNA hybridization using TYGS, which
242 reports that MSH1 (substrain DK1) is 82.5% (recommended $d_4$ formula) similar to *A. niigataensis*
243 DSM 7050. (Supplementary Table S1). Finally, ANI values against all available *Aminobacter*
244 genomes from NCBI (complete and incomplete assemblies; downloaded January 31, 2021),
245 showed an ANI of 98% against *A. niigataensis* DSM 7050 (Figure 4). Based on these analyses, we
246 reassign *Aminobacter* sp. MSH1 as *Aminobacter niigataensis* MSH1.

247

248 *Chromosomally encoded metabolic features of MSH1*

249 The chromosome of MSH1 possesses all genes required for glycolysis using the Embden-
250 Meyerhof pathway and additionally possesses all genes for glucose metabolism through the
251 Entner-Doudoroff pathway and the pentose phosphate pathway. It also contains all genes of the
252 tricarboxylic acid cycle. MSH1 was previously shown to grow slower on succinate and acetic acid
253 as carbon sources compared to glucose, fructose, and glycerol (43). MSH1 does not possess genes
254 involved in carbon fixation which rules out autotrophic growth. MSH1 further displays the
255 catechol *ortho*-cleavage pathway (44) and possesses genes for conversion of benzoate to catechol
256 allowing the organism to grow on benzoate which was confirmed by culturing the strain on
257 benzoate (data not shown). With regards to nitrogen metabolism, MSH1 contains a gene cluster

that encodes the transmembrane ammonium channel AmtB as well as its cognate protein GlnK (45) for controlling ammonium influx in response to the intracellular nitrogen status, indicating that MSH1 can use mineral ammonia as a nitrogen source directly from its environment. In addition, MSH1 encodes for proteins involved in nitrate transport (NrtA and NrtT). The corresponding genes are located upstream of genes for assimilatory nitrate reduction (*nasDEA*) to ammonium suggesting that MSH1 can also use nitrate as a nitrogen source. Finally, ammonia is also released from amino acid metabolism and is further incorporated in L-glutamate for biosynthesis. Furthermore, MSH1 contains a gene cluster which combines a periplasmic dissimilatory nitrate reductase (*napAB),* the membrane-bound cytochrome *c* (*napC*) that is involved in electron transfer from the quinol pool in the cytoplasmic membrane to NapAB, *nirK* (nitrate reductase) and *norBC* (nitrix oxide reductase). However, *narG,* encoding the cytoplasmatic oriented dissimilatory nitrate reductase, is lacking. Dissimilatory nitrate reductases are associated with the cell membrane, and are typically involved in energy acquisition, detoxification, and redox regulation (46) NarG, located at the cytoplasmatic side of the cell membrane, is the typical respiratory nitrate reductase though its function can be replaced by NapAB in cases coupled to formate oxidation (46). However, this is unlikely since MSH1 is unable to grow under nitrate reducing conditions (6). In addition, *nosZ* for reduction of nitrous oxide to dinitrogen (47) is missing. The exact function of the gene cluster containing *napABC*, *nirK* and *norBC* is yet unknown. Besides direct uptake, for sulfur metabolism, MSH1 possesses two nearby located gene clusters encoding the ABC transporter complex CysUWA involved in sulfate/thiosulfate import. One of the two clusters appears directed to the uptake of sulfate while the other to thiosulfate uptake, since they respectively are linked with *sbp* and *cysP* (48). Both genes encode for the periplasmic protein that delivers sulfate or thiosulfate to the ABC transporter for high affinity

uptake but Sbp binds sulfate and CysP thiosulfate. Furthermore, the chromosome contains all genes necessary for assimilatory sulfate reduction. The pathway reduces sulfate to sulfide involving ATP sulfurylase (CysND), adenosine 5'-phosphosulfate reductase (CysC), 3'-phosphoadenosine-5'-phosphosulfate reductase (CysH) and sulfite reductase (CisIJ). In addition, MSH1 contains *cysK* encoding O-acetylserine sulfhydrylase that incorporates sulfide into O-acetylserine to form cysteine (48). The assimilation of thiosulfate is less clear but MSH1 encodes for another homologue of CysK as well as several glutaredoxin proteins that are needed to incorporate thiosulfate in O-acetylserine and reductive cleavage reaction of its disulfide bond to form cysteine (48).

*Plasmids of MSH1*

Besides the previously described IncP1-β and *repABC* plasmids, pBAM1 and pBAM2 (7, 19), substrain DK1 harbors the five pUSP1-5 plasmids (Figure 2), while substrain MK1 lacks pUSP2, pUSP3, pUSP4, and pUSP5. Catabolic genes on pBAM1 and pBAM2 enable MSH1 to mineralize the groundwater micropollutant BAM and use it as a source of carbon, nitrogen, and energy for growth. The amidase BbdA on pBAM1 transforms BAM to 2,6-dichlorobenzoic acid (DCBA) (7) which is further metabolized by a series of catabolic enzymes encoded by pBAM2 (19, 49). As previously discussed (19), the gene *bbdI* encoding the gluthatione dependent thiolytic dehalogenase responsible for removal of one of the chlorines from BAM together with *bbdJ* encoding gluthatione reductase, occur on pBAM2 in three consecutive, perfect repeats followed by a fourth, imperfect repeat. This, together with the placement of the BAM degradation genes on two separate plasmids (pBAM1 and pBAM2) and the bordering of the catabolic gene clusters by remnants of insertion sequences and integrase genes, suggests that the BAM catabolic genes in

MSH1 have been acquired by horizonral gene transfer and then evolved to occur in their observed genomic organisation. In addition, pBAM2 has a considerably lower GC content of 56% compared to the chromosome and other plasmids which are between 60.0 and 64.4% (Table 2), which could indicate that pBAM2 was acquired from another, unknown, unrelated bacterium. It was previously shown that mineralization of DCBA is a common trait in bacteria in sand filters and soils, while BAM to DCBA conversion is the rate limiting step in BAM mineralization and is rare in microbial communities (50).

Like pBAM2, plasmids pUSP1, pUSP2, and pUSP3 belong to the *repABC* family. *repABC* replicons are known as typical genome components of *Alphaproteobacteria* species (51). The occurrence of more than one *repABC* replicon in one and the same genome has been described before and the plasmid family has been shown to exist of different incompatability groups. For instance, *Rhizobium etli* CFN42 has 6 *repABC* plasmids (52, 53).

Plasmids pBAM2, pUSP2, pUSP3, and pUSP4 contains Type IV secretion system (T4SS) genes (54), while pUSP1 does not. This indicates that pUSP1 is likely not self-transferable, unlike pBAM2, pUSP2, pUSP3, and pUSP4. Besides T4SS genes, plasmid pUSP4 contains a *mobABC* operon. The 31.6 kbp plasmid pUSP5 lacks conjugative transfer genes and appears to be a mobilizable plasmid with genes encoding a VirD4-like coupling protein and a TraA conjugative transfer relaxase likely involved in nicking at an *oriT* site and unwinding DNA before transfer. Furthermore, MOB-suite predicted that pBAM1, pUSP2, and pUSP4 have MOBP-type relaxase genes, while pUSP3 and pUSP5 have MOBQ-type relaxase genes. pBAM2 and pUSP1 were not predicted to have MOB-related genes.

*Specialized functions of plasmids pUSP1-5*

In Table 3, all CDS of the different plasmids are categorized according to COGs. Half of the CDS annotated on plasmid pUSP1 (322 CDS) and pUSP2 (346 CDS) are genes primarily associated with the transport and metabolism of amino acids (20% and 12%, resp.), carbohydrates (6% and 6%, resp.) and inorganic compounds (10% and 3%, resp.), and genes for energy production and conversion (9% and 8%, resp.). For the plasmids pUSP3, pUSP4, and pUSP5, CDS categorized under the same COGs are lower than 18%. Together, pUSP1 and pUSP2 accounts for about 17% of all genes in MSH1 related to amino acid, carbohydrate transport and metabolism, and energy production and conversion in MSH1. The transport systems encoded by pUSP1 and pUSP2 include multiple ABC-transporters for N and/or S-containing organic compounds. For amino acids, carbohydrates and inorganic compound metabolism and transport, ABC-type transport systems are predicted for polar amino acids (arginine, glutamine), branched chain amino acids, and multiple sugars. In addition, transport systems for spermidine/putrescine, taurine, aliphatic sulphonates, dipeptides, beta-methyl galactoside, polysialic acid, and phosphate were predicted. Putative functions could be assigned by Prokka to 64.2%, 56.8%, 27.4%, 42.2%, and 34.3% of CDS for pUSP1, pUSP2, pUSP3, pUSP5 and pUSP5, respectively. On pUSP1, found in both MSH1 substrains, multiple genes could be assigned to metabolic subsystems by RAST. These include folate biosynthesis, cytochrome oxidases and reductases, degradation of aromatic compounds (homogentisate pathway), ammonia assimilation, and several genes related to amino acid metabolism. Some of these functions on pUSP1 do not have functional analogs on the chromosome, which may help to explain why pUSP1 was not lost in substrain MK1, but the other pUSP plasmids were. On pUSP2, which is absent in MK1 substrain, some genes are predicted to be involved in acetyl-CoA fermentation to butyrate, creatine degradation, metabolism of butanol, fatty acids, and

nitrile, and a few miscellanoues functions. A large number of CDS on pUSP1 (19%), and pUSP2 (23%) are homologues to CDS on the chromosome and could be considered dispensable genes. However, although these CDS might be considered homologues, their functionality might differ considerably in terms of substrate specificity and kinetics.

Besides genes encoding conjugative transfer, plasmid replication, and plasmid stability functions, most genes on plasmids pUSP3, pUSP4, and pUSP5 could not be annotated with a function. However, several genes on pUSP3 may have functions related to metabolism of sugars, including inositol and mannose which were not tested in an earlier growth optimization experiment (43). On pUSP4, genes encoding a transmembrane amino acid transporter are situated next to an aspartate ammonia-lyase-encoding gene that enables conversion between aspartate and fumarate that may enter the tricarboxylic acid cycle, as described above. A cytochrome bd-type quinol oxidase, encoded by two subunit genes on pUSP5, also occurs in some nitrogen-fixing bacteria where it is responsible for removing oxygen in microaerobic conditions. Furthermore, a pseudoazurin type I blue copper electron-transfer protein is encoded by a gene on pUSP5, that may act as an electron donor in a denitrification pathway. A chromate transporter, ChrA, encoded by a gene on pUSP5 may confer resistance to chromate. Future studies should look into whether the lack of plasmids pUSP2-5 in substrain MK1 has phenotypic consequences, with regards to the predicted functions, including metabolism of sugars and aspartate, nitrogen metabolism, and resistance to chromate.

372 *Plasmid stability and chromosome polyploidy*

373 The Illumina sequencing coverage of several plasmids relative to the chromosome (except for
374 pBAM1) was lower than one, i.e., approximately 0.3 to 0.6 per chromosome. This suggests that
375 either not all cells (only three to six out of ten) contain a copy of the same plasmid due to plasmid
376 loss or that there are multiple copies of the chromosome. Previously, in the MK1 substrain, we
377 observed that pBAM2 is not always perfectly inherited by the daughter cells in cultures grown in
378 R2B and R2B containing BAM (15). To observe whether plasmid instability explained the copy
379 number relative to the chromosome in the sequenced cultures, sequencing was performed directly
380 on the cryo stock as well as on colonies directly derived from this, mimicking the sequenced cell
381 preparation for whole genome sequencing. We hypothesized that if certain plasmids are not stably
382 inherited (i.e. those with copy numbers 0.3 to 0.6), only part of the cell population will habour
383 those plasmids and picking of multiple colonies from a plate will result in picking of some colonies
384 that have lost one or more plasmids.

385 MSH1 was sequenced directly from the cryostock, from a single colony picked from R2A plates
386 after spreading the cryostock, and from the broth R2B culture that had been inoculated with the
387 same single colony from cryostock. Moreover, after spreading the latter R2B culture on an R2A
388 plate, an additional 14 MSH1 colonies were picked for sequencing. Taking into account a plasmid
389 coverage of 0.3 – 0.6 per chromosome, we expect that around half of the colonies would have lost
390 one or more of the plasmids in the case of poor inheritance. However, only one of the colonies
391 showed loss of a plasmid, i.e., plasmid pUSP1 (Figure 5) indicating polyploidy of the chromosome
392 rather than unstable inheritance of plasmids. The loss of *repABC* megaplasmid pUSP1 shows that
393 the possible metabolic features encoded by genes on pUSP1, as described above, are not essential
394 for growth under these conditions, although, remarkably this is the only pUSP plasmid still present

in substrain MK1. Interestingly, the plasmid/chromosome-ratio varied according to the growth medium from which DNA was isolated. When growing in R2B (broth), e.g. as done for DNA extraction for genome sequencing and from cryostock and R2B culture (first and third green rings, Figure 6), all plasmids, except pBAM1, have a copy number lower than one per chromosome. When DNA was extracted from colonies grown on R2A plates (though resuspended in PBS prior to DNA extraction), plasmid copy numbers were approx. one per chromosome, except for pBAM1 which has a copy number of approx. 2.5 per chromosome.

Except for the single loss of pUSP1, nothing here indicates unstable maintenance of plasmids and subsequent loss. Instead, our results indicate that MSH1 regulates the chromosome copy number according to whether it grows as planktonic bacteria or fixed on an agar plate. The results shown here can be explained by MSH1 being polyploid with regards to its chromosome when growing in broth media. Single-copy plasmids (e.g. pBAM2, pUSP1-5) will thereby have copy numbers lower than one relative to the chromosome, when growing in broth R2B. Polyploidy in prokaryotes have been described before, including in *Deinococcus*, *Borrelia*, *Azotobacter*, *Neisseria*, *Buchnera*, and *Desulfovibrio* (55) and may be quite overlooked in many other bacteria. *E. coli* in stationary phase was shown to have two chromosome copies after growing in rich, complex medium, but only 60% of the cells had two copies in stationary phase after slower growth in a synthetic medium (55). It was suggested that monoploidy is not typical for proteobacteria, and that many bacteria are polyploid when growing in exponential phase (55). Possible advantages offered by polyploidy include resistance to DNA damage and mutations, global regulation of gene expression by changing chromosome copy number, and finally polyploidy may enable heterozygosity in bacteria where genes mutate to cope with challenging condition while preserving a copy of the original genes. Despite the stability of the plasmids in MSH1, the MSH1 substrain MK1 lacks plasmids

418 pUSP2-5 and a loss of pBAM2 was previously observed (15). Although pBAM2 encodes its own
419 T4SS, the multiple loss of pBAM2 and pUSP2-5 in MK1 could be hypothetically explained by
420 some uncharacterized plasmid codependence, where one loss leads to another. The dynamics of
421 plasmid loss that has led to formation of substrain MK1 are still unknown.

422 ## Conclusions

423 The full genome of *Aminobacter* sp. MSH1, re-identified here as *Aminobacter niigataensis* MSH1,
424 consisting of a chromosome and seven plasmids, was determined combining both Nanopore and
425 Illumina sequencing. Two smaller plasmids pBAM1 and pBAM2 were previously identified
426 carrying the catabolic genes required for mineralization of the groundwater micropollutant BAM.
427 Both the chromosome and the other five plasmids are described here for the first time. A plasmid
428 stability experiment showed that most plasmids were stably maintained, with exception of a single
429 loss event of plasmid pUSP1. Instead, the results indicate that MSH1 has a polyploid chromosome
430 when growing in broth, thereby reducing plasmid copy numbers per chromosome to below one.
431 When comparing the original strain MSH1 (DK1) and substrain MK1, we observed that plasmids
432 pUSP2, pUSP3, pUSP4, and pUSP5 were below detection limits in MK1. Substrain MK1 may
433 previously have lost these plasmids but maintained pUSP1, pBAM1, and pBAM2, thereby
434 retaining its capacity to degrade BAM. Future studies on growth and degradation kinetics of the
435 MSH1 and its substrain MK1 lacking several plasmids, can reveal if plasmids pUSP2-5 harbour
436 unknown (favorable) functions or if they impose a metabolic burden on MSH1. This will help to
437 elucidate which substrain is preferable for bioaugmentation.

## Funding

This project (LHH, LEJ, OH, and JAA) was funded by MEM2BIO (Innovation Fund Denmark, contract number 5157-00004B) at Aarhus University and DS by the KU Leuven C1 project no. C14/15/043 and the BELSPO IAP-project μ-manager no. P7/25 at KU Leuven. BH was supported by postdoctoral fellowship grant 12Q0218N and CL by an SB-FWO PhD fellowship 1S64718N. TKN was supported by AUFF NOVA project ORIGENE.

## Authors' contributions

LHH, TKN, BH and DS initiated, planned, and funded the project. BH and TKN wrote the initial draft manuscript. BH, TKN, and CL performed genome sequencing, assembly annotation, and data analyses. OH performed the plasmid stability experiment. VvN, RL, DS, LEJ, JA, and LHH critically reviewed the paper, assisted in data interpretation, and coordinated experiments.

## References

1. Schwarzenbach RP, Escher BI, Fenner K, Hofstetter TB, Johnson CA, von Gunten U, Wehrli B. 2006. The challenge of micropollutants in aquatic systems. Science (80- ) 313:1072–1077.

2. EU. 1998. Council Directive 98/83/EC of 3 November 1998 on the quality of water intended for human consumption. Counc Eur Union.

3. Benner J, Helbling DE, Kohler HP, Wittebol J, Kaiser E, Prasse C, Ternes TA, Albers CN, Aamand J, Horemans B, Springael D, Walravens E, Boon N. 2013. Is biological treatment a viable alternative for micropollutant removal in drinking water treatment processes? Water Research 47(16):5955-5976

459 4. Vandermaesen J, Horemans B, Bers K, Vandermeeren P, Herrmann S, Sekhar A,
460 Seuntjens P, Springael D. 2016. Application of biodegradation in mitigating and
461 remediating pesticide contamination of freshwater resources: state of the art and
462 challenges for optimization. Appl Microbiol Biotechnol 100:7361-7376.

463 5. Björklund E, Anskjær GG, Hansen M, Styrishave B, Halling-Sørensen B. 2011. Analysis
464 and environmental concentrations of the herbicide dichlobenil and its main metabolite 2,6-
465 dichlorobenzamide (BAM): A review. Sci Total Environ 409:2343-2356.

466 6. Sørensen SR, Holtze MS, Simonsen A, Aamand J. 2007. Degradation and mineralization
467 of nanomolar concentrations of the herbicide dichlobenil and Its persistent metabolite 2,6-
468 dichlorobenzamide by *Aminobacter* spp. isolated from dichlobenil-treated soils. Appl
469 Environ Microbiol 73:399–406.

470 7. T'Syen J, Tassoni R, Hansen L, Sorensen SJ, Leroy B, Sekhar A, Wattiez R, De Mot R,
471 Springael D. 2015. Identification of the amidase BbdA that initiates biodegradation of the
472 groundwater micropollutant 2,6-dichlorobenzamide (BAM) in *Aminobacter* sp. MSH1.
473 Environ Sci Technol 49:11703–11713.

474 8. Horemans B, Raes B, Vandermaesen J, Simanjuntak Y, Brocatus H, T'Syen J, Degryse J,
475 Boonen J, Wittebol J, Lapanje A, Sorensen SR, Springael D. 2016. Biocarriers improve
476 bioaugmentation efficiency of a rapid sand filter for the treatment of 2,6-
477 dichlorobenzamide (BAM)-contaminated drinking water. Environ Sci Technol 51:1616–
478 1625.

479 9. Albers CN, Feld L, Ellegaard-Jensen L, Aamand J. 2015. Degradation of trace
480 concentrations of the persistent groundwater pollutant 2,6-dichlorobenzamide (BAM) in

bioaugmented rapid sand filters. Water Res 83:61–70.

10. Albers CN, Jacobsen OS, Aamand J. 2013. Using 2,6-dichlorobenzamide (BAM) degrading *Aminobacter* sp. MSH1 in flow through biofilters—initial adhesion and BAM degradation potentials. Appl Microbiol Biotechnol 98:957–967.

11. Ellegaard-Jensen L, Albers CN, Aamand J. 2016. Protozoa graze on the 2,6-dichlorobenzamide (BAM)-degrading bacterium *Aminobacter* sp. MSH1 introduced into waterworks sand filters. Appl Microbiol Biotechnol 1–9.

12. Ellegaard-Jensen L, Horemans B, Raes B, Aamand J, Hansen LH. 2017. Groundwater contamination with 2,6-dichlorobenzamide (BAM) and perspectives for its microbial removal. Appl Microbiol Biotechnol 101(13):5235-5245.

13. Ellegaard-Jensen L, Schostag MD, Nikbakht Fini M, Badawi N, Gobbi A, Aamand J, Hansen LH. 2020. Bioaugmented Sand Filter Columns Provide Stable Removal of Pesticide Residue From Membrane Retentate. Front. Water.

14. Sekhar A, Horemans B, Aamand E, Vanhaeke L, Hofkens J, Springael D. 2013. Evaluation of the biofilm forming capacity of the 2, 6-dichlorobenzamide (BAM) degrading *Aminobacter* sp. strain MSH1 at macropollutant and micropollutant BAM concentrations. Commun Agric Appl Biol Sci. 2013;78(1):31-6

15. Horemans B, Raes B, Brocatus H, T'Syen J, Rombouts C, Vanhaecke L, Hofkens J, Springael D. 2017. Genetic (in)stability of 2,6-dichlorobenzamide catabolism in *Aminobacter* sp. strain MSH1 biofilms under carbon starvation conditions. Appl Environ Microbiol 83(11):e00137-17.

16. Martin M. 2014. Cutadapt removes adapter sequences from high-throughput sequencing

reads. EMBnet.journal.

17. Schubert M, Lindgreen S, Orlando L. 2016. AdapterRemoval v2: Rapid adapter trimming, identification, and read merging. BMC Res Notes 9:88.

18. Wick RR, Judd LM, Gorrie CL, Holt KE. 2017. Unicycler: Resolving bacterial genome assemblies from short and long sequencing reads. PLoS Comput Biol 13(6):e1005595.

19. T'Syen J, Raes B, Horemans B, Tassoni R, Leroy B, Lood C, van Noort V, Lavigne R, Wattiez R, Kohler H-PE, Springael D. 2018. Catabolism of the groundwater micropollutant 2,6-dichlorobenzamide beyond 2,6-dichlorobenzoate is plasmid encoded in *Aminobacter* sp. MSH1. Appl Microbiol Biotechnol 102:7963–7979.

20. Andrews S. 2010. FastQC - A quality control tool for high throughput sequence data. http://www.bioinformatics.babraham.ac.uk/projects/fastqc/. Babraham Bioinformatics.

21. Bushnell B, Rood J, Singer E. 2017. BBMerge – Accurate paired shotgun read merging via overlap. PLoS One 12(10):e0185056.

22. Seemann T. 2014. Prokka: Rapid prokaryotic genome annotation. Bioinformatics.

23. Krogh A, Larsson B, von Heijne G, Sonnhammer ELL. 2001. Predicting transmembrane protein topology with a hidden markov model: application to complete genomes. J Mol Biol 305:567–580.

24. Huerta-Cepas J, Forslund K, Coelho LP, Szklarczyk D, Jensen LJ, von Mering C, Bork P. 2017. Fast Genome-Wide Functional Annotation through Orthology Assignment by eggNOG-Mapper. Mol Biol Evol 34:2115–2122.

25. Blom J, Albaum SP, Doppmeier D, Pühler A, Vorhölter F-J, Zakrzewski M, Goesmann A. 2009. EDGAR: A software framework for the comparative analysis of prokaryotic

525 genomes. BMC Bioinformatics 10:154.

526 26. Karp PD, Latendresse M, Paley SM, Krummenacker M, Ong QD, Billington R, Kothari
527 A, Weaver D, Lee T, Subhraveti P, Spaulding A, Fulcher C, Keseler IM, Caspi R. 2016.
528 Pathway Tools version 19.0 update: software for pathway/genome informatics and
529 systems biology. Brief Bioinform 17:877–890.

530 27. Aziz RK, Bartels D, Best A, DeJongh M, Disz T, Edwards RA, Formsma K, Gerdes S,
531 Glass EM, Kubal M, Meyer F, Olsen GJ, Olson R, Osterman AL, Overbeek RA, McNeil
532 LK, Paarmann D, Paczian T, Parrello B, Pusch GD, Reich C, Stevens R, Vassieva O,
533 Vonstein V, Wilke A, Zagnitko O. 2008. The RAST Server: Rapid annotations using
534 subsystems technology. BMC Genomics 9:75.

535 28. Krzywinski MI, Schein JE, Birol I, Connors J, Gascoyne R, Horsman D, Jones SJ, Marra
536 MA. 2009. Circos: An information aesthetic for comparative genomics. Genome Res
537 19:1639-1645.

538 29. Kumar S, Stecher G, Li M, Knyaz C, Tamura K. 2018. MEGA X: Molecular Evolutionary
539 Genetics Analysis across Computing Platforms. Mol Biol Evol 35:1547–1549.

540 30. Sievers F, Wilm A, Dineen D, Gibson TJ, Karplus K, Li W, Lopez R, McWilliam H,
541 Remmert M, Söding J, Thompson JD, Higgins DG. 2011. Fast, scalable generation of
542 high-quality protein multiple sequence alignments using Clustal Omega. Mol Syst Biol
543 7:539.

544 31. Lethiec F, Gascuel O, Duroux P, Guindon S. 2005. PHYML Online—a web server for fast
545 maximum likelihood-based phylogenetic inference. Nucleic Acids Res 33:W557–W559.

546 32. Meier-Kolthoff JP, Göker M. 2019. TYGS is an automated high-throughput platform for

state-of-the-art genome-based taxonomy. Nat Commun 10:2182.

33. Jain C, Rodriguez-R LM, Phillippy AM, Konstantinidis KT, Aluru S. 2018. High throughput ANI analysis of 90K prokaryotic genomes reveals clear species boundaries. Nat Commun 9:5114.

34. Kolde R. 2015. pheatmap : Pretty Heatmaps. R package version 1.0.12. R Package version 108.

35. Darling ACE, Mau B, Blattner FR, Perna NT. 2004. Mauve: Multiple alignment of conserved genomic sequence with rearrangements. Genome Res 7:1394-403.

36. Robertson J, Nash JHE. 2018. MOB-suite: software tools for clustering, reconstruction and typing of plasmids from draft assemblies. Microb genomics 4:8.

37. Bolger AM, Lohse M, Usadel B. 2014. Trimmomatic: A flexible trimmer for Illumina Sequence Data. Bioinformatics 30(15):2114-2120.

38. Li H.; Durbin R. 2009. Fast and accurate short read alignment with Burrows–Wheeler transform. Bioinformatics 25:1754–1760.

39. Li H, Handsaker B, Wysoker A, Fennell T, Ruan J, Homer N, Marth G, Abecasis G, Durbin R. 2009. The Sequence Alignment/Map format and SAMtools. Bioinformatics 25(16):2078-9.

40. Quinlan AR, Hall IM. 2010. BEDTools: a flexible suite of utilities for comparing genomic features. Bioinformatics 26:841–842.

41. Olasz F, Stalder R, Arber W. 1993. Formation of the tandem repeat (IS 30)2 and its role in IS 30-mediated transpositional DNA rearrangements. MGG Mol Gen Genet 239:177-187.

568 42. Olasz F, Farkas T, Kiss J, Arini A, Arber W. 1997. Terminal inverted repeats of insertion
569 sequence IS30 serve as targets for transposition. J Bacteriol 179(23):7551-8.

570 43. Schultz-Jensen N, Knudsen BE, Frkova Z, Aamand J, Johansen T, Thykaer J, Sørensen
571 SR. 2014. Large-scale bioreactor production of the herbicide-degrading *Aminobacter* sp.
572 strain MSH1. Appl Microbiol Biotechnol 98:2335-2344.

573 44. Harayama S, Mermod N, Rekik M, Lehrbach PR, Timmis KN. 1987. Roles of the
574 divergent branches of the meta-cleavage pathway in the degradation of benzoate and
575 substituted benzoates. J Bacteriol 169(2):558-64.

576 45. Zheng L, Kostrewa D, Bernèche S, Winkler FK, Li XD. 2004. The mechanism of
577 ammonia transport based on the crystal structure of AmtB of *Escherichia coli*. Proc Natl
578 Acad Sci U S A 101(49):17090-17095.

579 46. Sparacino-Watkins C, Stolz JF, Basu P. 2014. Nitrate and periplasmic nitrate reductases.
580 Chem Soc Rev 43(2):676-706.

581 47. Bedzyk L, Wang T, Ye RW. 1999. The periplasmic nitrate reductase in *Pseudomonas* sp.
582 strain G-179 catalyzes the first step of denitrification. J Bacteriol 181(9):2802-6.

583 48. Kawano Y, Suzuki K, Ohtsu I. 2018. Current understanding of sulfur assimilation
584 metabolism to biosynthesize l-cysteine and recent progress of its fermentative
585 overproduction in microorganisms. Appl Microbiol Biotechnol 102(19):8203-8211.

586 49. Raes B, Horemans B, Rentsch D, T'Syen J, Ghequire M, De Mot R, Wattiez R, Kohler H-
587 P, Springael D. 2019. *Aminobacter* sp. MSH1 mineralises the groundwater micropollutant
588 2,6-dichlorobenzamide through a unique chlorobenzoate catabolic pathway. Environ Sci
589 Technol 53:10146–10156.

590 50. Vandermaesen J, Horemans B, Degryse J, Boonen J, Walravens E, Springael D. 2016.
591 Mineralization of the Common Groundwater Pollutant 2,6-Dichlorobenzamide (BAM)
592 and its Metabolite 2,6-Dichlorobenzoic Acid (2,6-DCBA) in Sand Filter Units of Drinking
593 Water Treatment Plants. Environ Sci Technol 50(18):10114-10122.

594 51. Cevallos MA, Cervantes-Rivera R, Gutiérrez-Ríos RM. 2008. The *repABC* plasmid
595 family. Plasmid 60(1):19-37.

596 52. González V, Santamaría RI, Bustos P, Hernández-González I, Medrano-Soto A, Moreno-
597 Hagelsieb G, Janga SC, Ramírez MA, Jiménez-Jacinto V, Collado-Vides J, Dávila G.
598 2006. The partitioned *Rhizobium etli* genome: Genetic and metabolic redundancy in seven
599 interacting replicons. Proc Natl Acad Sci U S A 103(10):3834-3839.

600 53. Castillo-Ramírez S, Vázquez-Castellanos JF, González V, Cevallos MA. 2009. Horizontal
601 gene transfer and diverse functional constrains within a common replication-partitioning
602 system in Alphaproteobacteria: The *repABC* operon. BMC Genomics 10:536.

603 54. Cascales E, Christie PJ. 2003. The versatile bacterial type IV secretion systems. Nat Rev
604 Microbiol 1:137–149.

605 55. Pecoraro V, Zerulla K, Lange C, Soppa J. 2011. Quantification of Ploidy in Proteobacteria
606 Revealed the Existence of Monoploid, (Mero-)Oligoploid and Polyploid Species. PLoS
607 One 6:e16392.

608 56. Albers P, Lood C, Özturk B, Horemans B, Lavigne R, van Noort V, De Mot R, Marchal
609 K, Sanchez-Rodriguez A, Springael D. 2018. Catabolic task division between two near-
610 isogenic subpopulations co-existing in a herbicide-degrading bacterial consortium:
611 consequences for the interspecies consortium metabolic model. Environ Microbiol 20:85–

612 96.

613

# Tables

**Table 1.** Genome accession codes

| Label | Size (Mb) | GC (%) | Topology | INSDC identifier | RefSeq ID |
|---|---|---|---|---|---|
| Chromosome | 5.30 | 63.2 | Circular | CP028968.1(CP026265.1)* | NZ_CP028968.1(NZ_CP026265.1)* |
| Plasmid 1 pBAM1 | 0.04 | 64.4 | Circular | CP028967.1(CP026268.1)* | NZ_CP028967.1(NZ_CP026268.1)* |
| Plasmid 2 pBAM2 | 0.05 | 56.0 | Circular | CP028966.1(CP026267.1)* | NZ_CP028966.1(NZ_CP026267.1)* |
| Plasmid 3 pUSP1 | 0.37 | 63.1 | Circular | CP028969.1(CP026266.1)* | NZ_CP028969.1(NZ_CP026266.1)* |
| Plasmid 4 pUSP2 | 0.37 | 60.1 | Circular | CP028970.1 | NZ_CP028970.1 |
| Plasmid 5 pUSP3 | 0.10 | 60.5 | Circular | CP028971.1 | NZ_CP028971.1 |
| Plasmid 6 pUSP4 | 0.06 | 61.9 | Circular | CP028972.1 | NZ_CP028972.1 |
| Plasmid 7 pUSP5 | 0.03 | 62.9 | Circular | CP028973.1 | NZ_CP028973.1 |

* INSDC identifier and RefSeqID of KU Leuven substrain MK1 submission in brackets

**Table 2**. Genome statistics based on substrain MK1.

| Attribute | Value | % of Total |
|---|---|---|
| Genome size (bp) | 6321606 | 100.0 |
| DNA coding (bp) | 5587258 | 88.4 |
| DNA G+C (bp) | 3976162 | 62.9 |
| DNA scaffolds | 8 | 100.0 |
| Total genes | 6257 | 100.0 |
| Protein coding genes | 6004 | 96.0 |
| RNA genes | 63 | 1.0 |
| Pseudo genes | 190 | 3.0 |
| Genes with function prediction | 5182 | 75.9 |
| Genes assigned to COGs | 3890 | 62.2 |

| | | |
|---|---|---|
| Genes with Pfam domains | 5006 | 81.0 |
| Genes with signal peptides | 565 | 9.0 |
| Genes with transmembrane helices | 1423 | 22.7 |
| CRISPR repeats | 0 | 0.0 |

628 **Table 3**. Percentage of genes associated with general COG functional categories in genome and replicons.

| Code | Description | Total | Chr | pBAM1 | pBAM2 | pUSP1 | pUSP2 | pUSP3 | pUSP4 | pUSP5 |
|---|---|---|---|---|---|---|---|---|---|---|
| J | Translation, ribosomal structure and biogenesis | 2.9% | 3% | 0% | 0% | 2% | 1% | 0% | 0% | 0% |
| A | RNA processing and modification | 0.0% | 0% | 0% | 0% | 0% | 0% | 0% | 0% | 0% |
| K | Transcription | 7.3% | 7% | 5% | 9% | 10% | 7% | 9% | 5% | 18% |
| L | Replication, recombination and repair | 4.9% | 4% | 20% | 21% | 2% | 12% | 14% | 16% | 18% |
| B | Chromatin structure and dynamics | 0.1% | 0% | 0% | 0% | 0% | 0% | 0% | 0% | 0% |
| D | Cell cycle control, Cell division, chromosome partitioning | 0.7% | 1% | 2% | 2% | 2% | 1% | 2% | 3% | 6% |
| V | Defense mechanisms | 1.0% | 1% | 0% | 0% | 0% | 1% | 0% | 2% | 0% |
| T | Signal transduction mechanisms | 2.5% | 3% | 0% | 0% | 1% | 1% | 0% | 3% | 3% |
| M | Cell wall/membrane biogenesis | 3.8% | 4% | 0% | 0% | 2% | 1% | 2% | 2% | 0% |
| N | Cell motility | 0.6% | 1% | 0% | 0% | 0% | 0% | 0% | 0% | 0% |
| U | Intracellular trafficking and secretion | 2.5% | 2% | 24% | 17% | 0% | 3% | 11% | 22% | 3% |
| O | Posttranslational modification, protein turnover, chaperones | 3.0% | 3% | 0% | 17% | 1% | 0% | 0% | 0% | 0% |
| C | Energy production and conversion | 5.1% | 5% | 2% | 2% | 9% | 8% | 5% | 2% | 12% |
| G | Carbohydrate transport and metabolism | 4.1% | 4% | 0% | 6% | 6% | 6% | 2% | 2% | 0% |
| E | Amino acid transport and metabolism | 9.8% | 9% | 2% | 2% | 20% | 12% | 7% | 6% | 0% |
| F | Nucleotide transport and metabolism | 1.6% | 2% | 0% | 0% | 1% | 0% | 0% | 0% | 0% |
| H | Coenzyme transport and metabolism | 2.3% | 3% | 0% | 0% | 2% | 1% | 0% | 0% | 0% |
| I | Lipid transport and metabolism | 2.3% | 2% | 0% | 0% | 2% | 5% | 3% | 0% | 3% |
| P | Inorganic ion transport and metabolism | 5.8% | 6% | 0% | 0% | 10% | 3% | 0% | 0% | 3% |
| Q | Secondary metabolites biosynthesis, transport and catabolism | 1.9% | 2% | 5% | 4% | 5% | 6% | 1% | 0% | 0% |
| R | General function prediction only | 0.0% | 0% | 0% | 0% | 0% | 0% | 0% | 0% | 0% |
| S | Function unknown | 20.7% | 21% | 10% | 13% | 17% | 21% | 17% | 5% | 21% |
| - | Not in COGs | 16.9% | 17% | 29% | 8% | 9% | 12% | 27% | 33% | 15% |
| **CDS** | | **6237** | **5277** | **41** | **53** | **322** | **346** | **100** | **63** | **34** |

629

# Figures

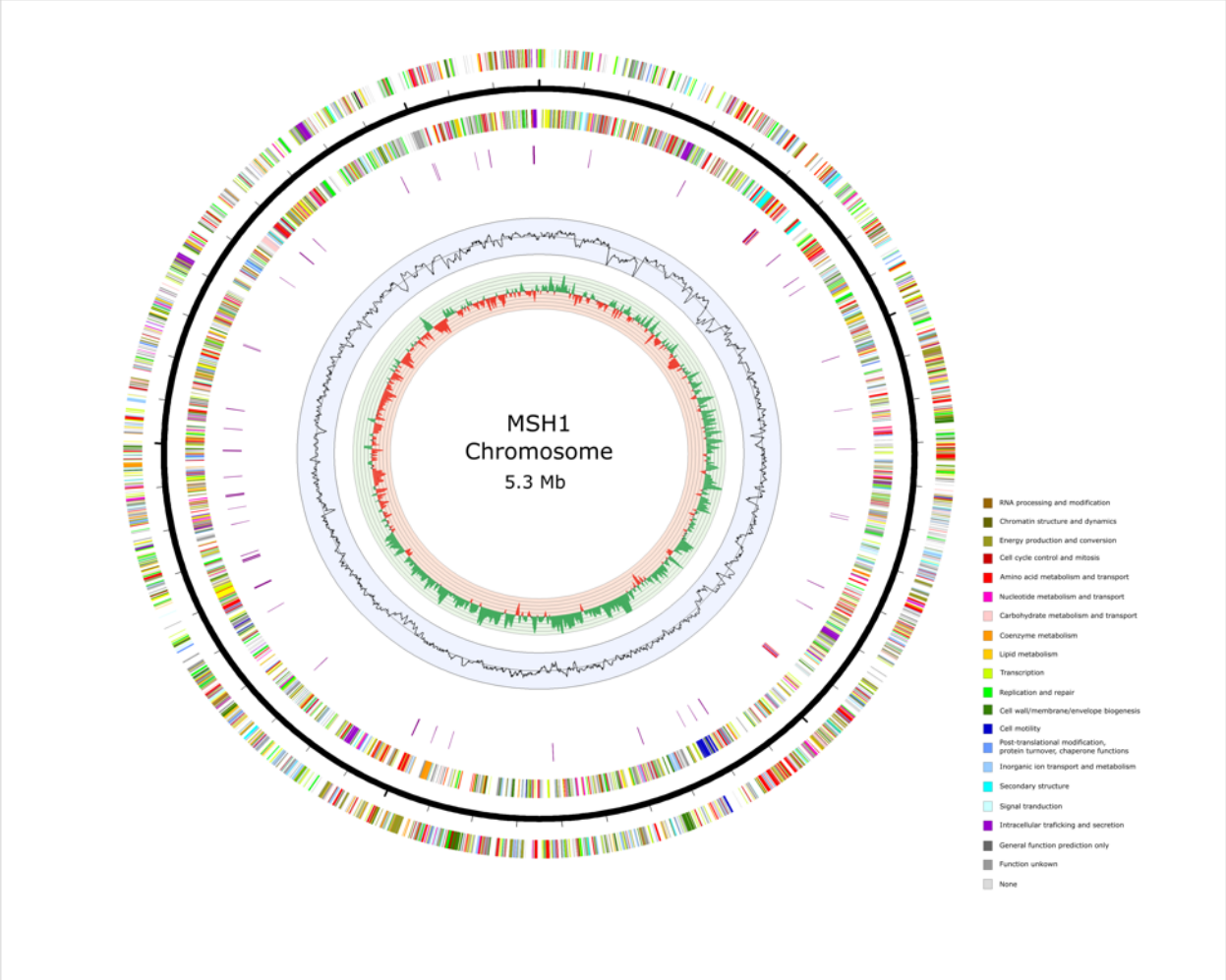


**Figure 1.** Circular view of the chromosome of *Aminobacter* sp. MSH1. From outer to inner circle: CDS on leading strand, scale (ticks: 100 kb), CDS on lagging strand, tRNA (purple) and rRNA (red) (only chromosome), GC plot and GC skew (>0: green, <0: red). CDS are colored according to COG functional categories determined with EggNOG mapper 4.5.1.

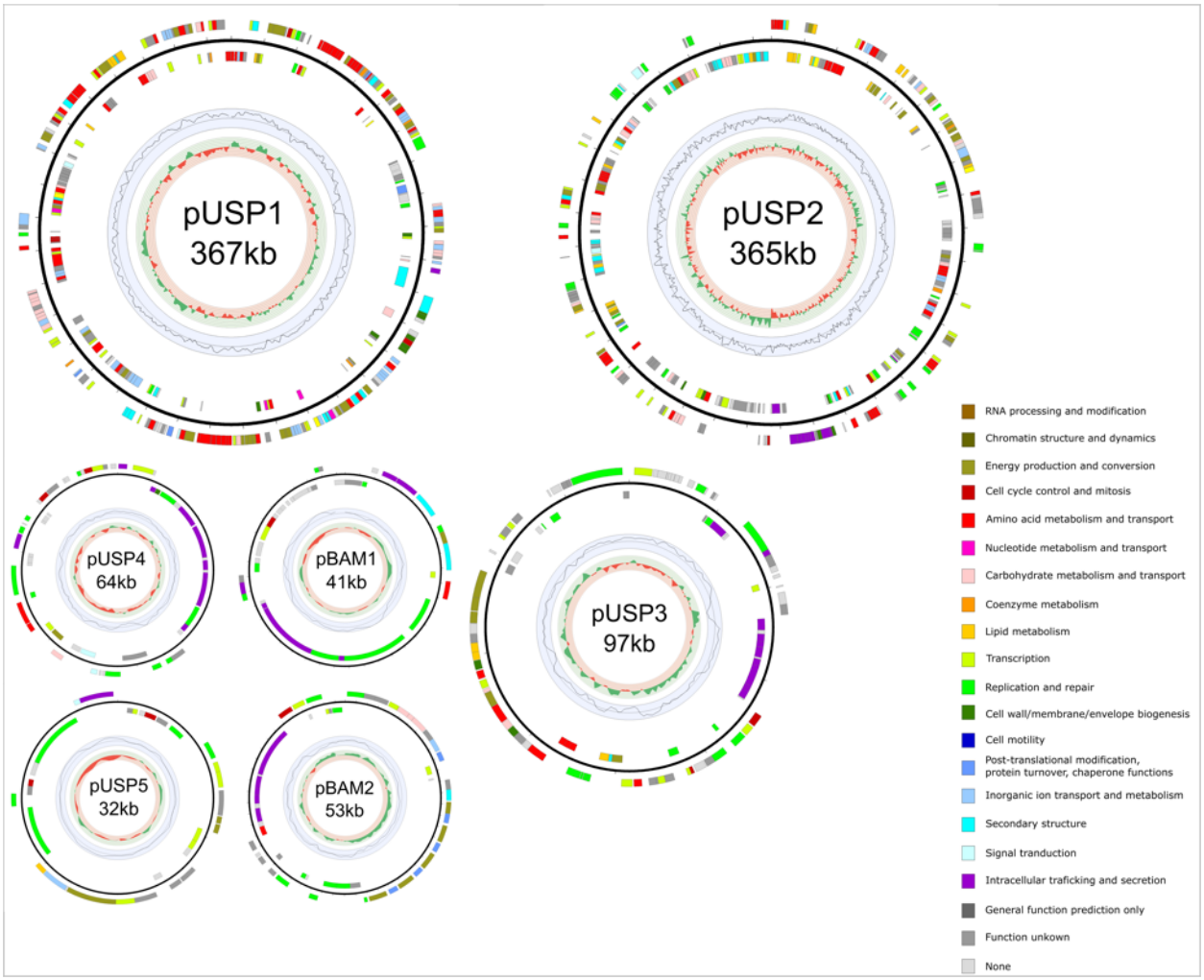


**Figure 2.** Circular view of the plasmids of the newly assigned *Aminobacter niigataensis* MSH1. From outer to inner circle: CDS on leading strand, scale (ticks: 100 kb), CDS on lagging strand, GC plot and GC skew (>0: green, <0: red). CDS are colored according to COG functional categories determined with EggNOG mapper 4.5.1. The KU Leuven substrain MK1 lacks plasmids pUSP2-5.

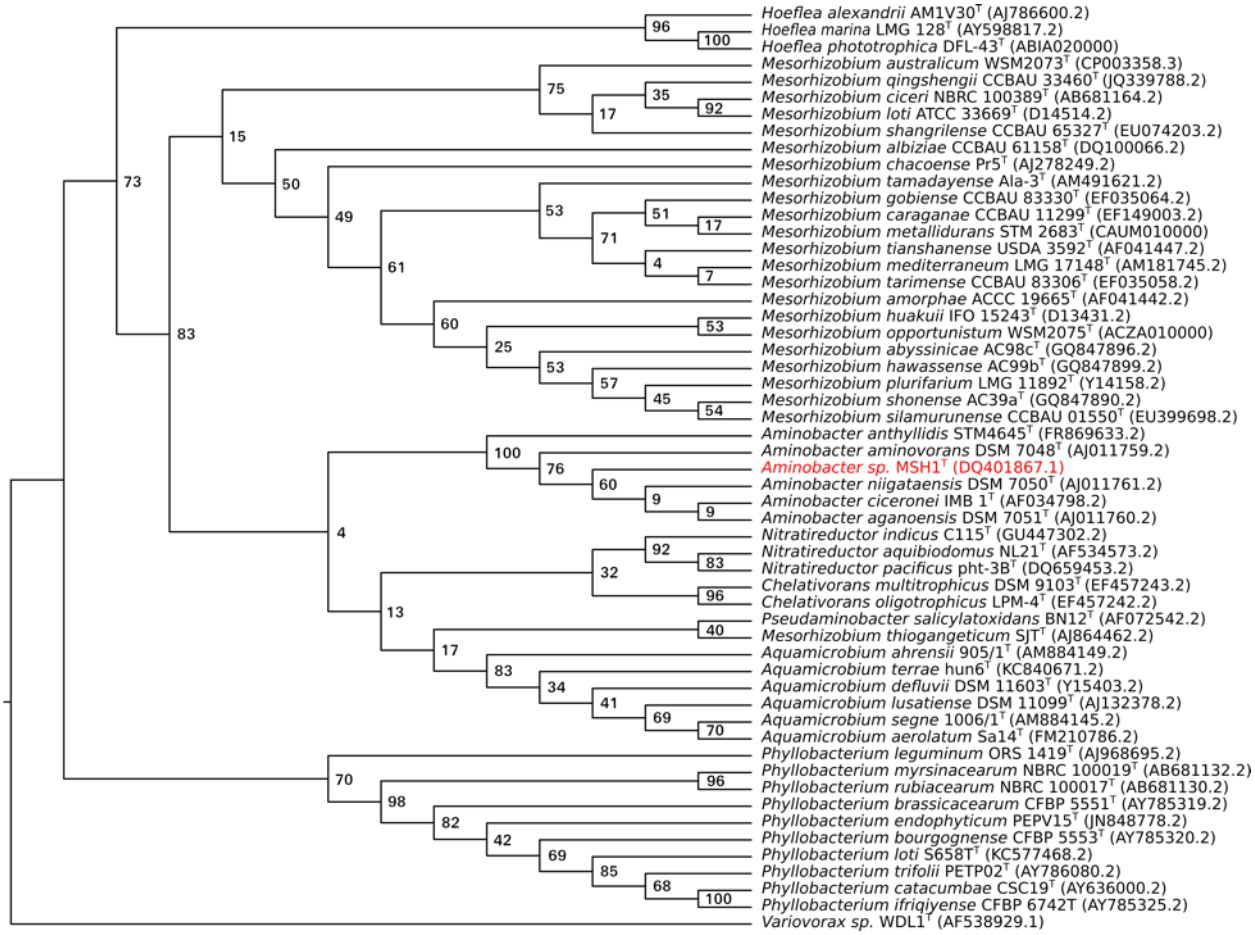


**Figure 3.** Phylogenetic relationships of *Aminobacter niigataensis* MSH1 based on the 16S rRNA gene sequence. Maximum likehood tree visualized as a cladogram with bootstrap values. This tree was created from a clustal-omega (30) multiple sequence alignment using 16S rRNA genes from the set of type strains available in the *Phyllobacteriaceae* family (NCBI accession numbers between parenthesis). The tree was inferred using PhyML (31) with a GTR substitution model and a calculation of branch support values (bootstrap value of 1000). The *Variovorax* sp. strain WDL1 was used as an outgroup (56).

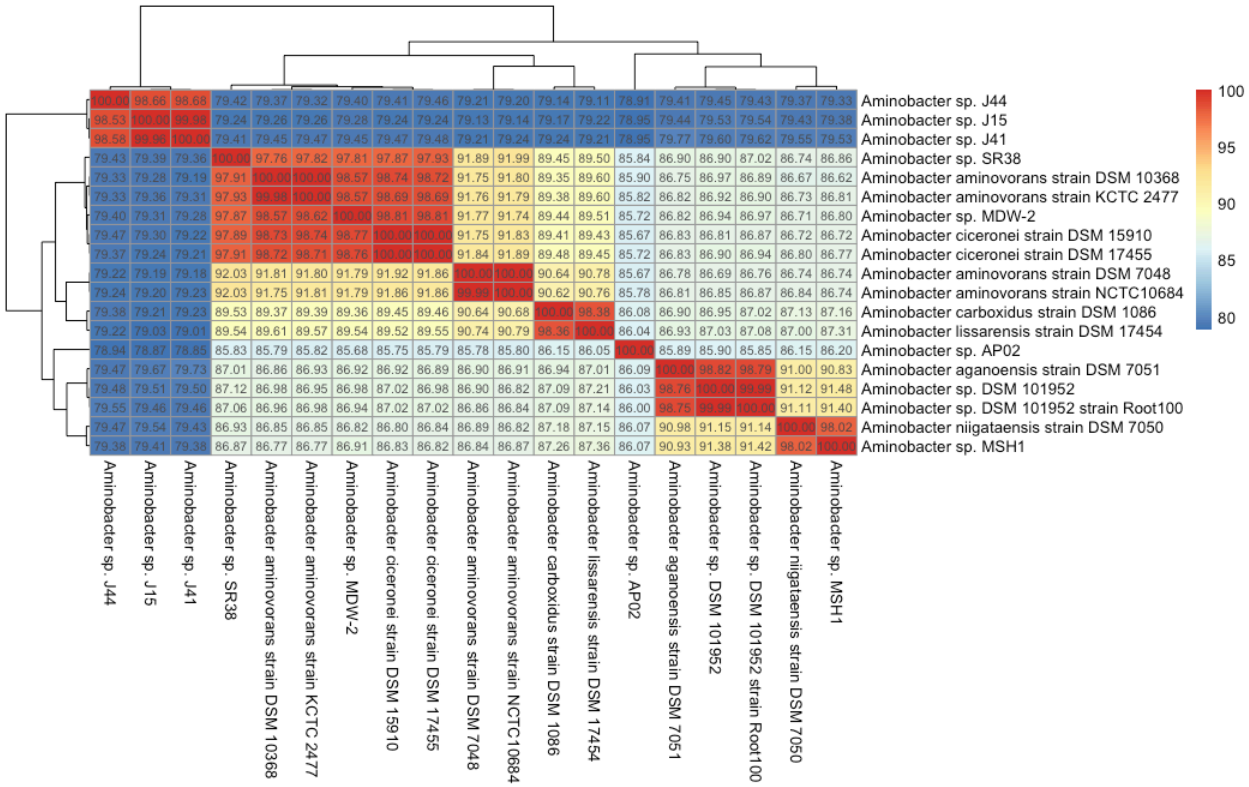


650

651 **Figure 4.** Heatmap of ANI values for all available *Aminobacter* genomes from NCBI (downloaded

652 January 31, 2021). Genomes are clustered using hierarchical clustering of ANI values, as implemented in

653 the R package "pheatmap" (v1.0.12).

654

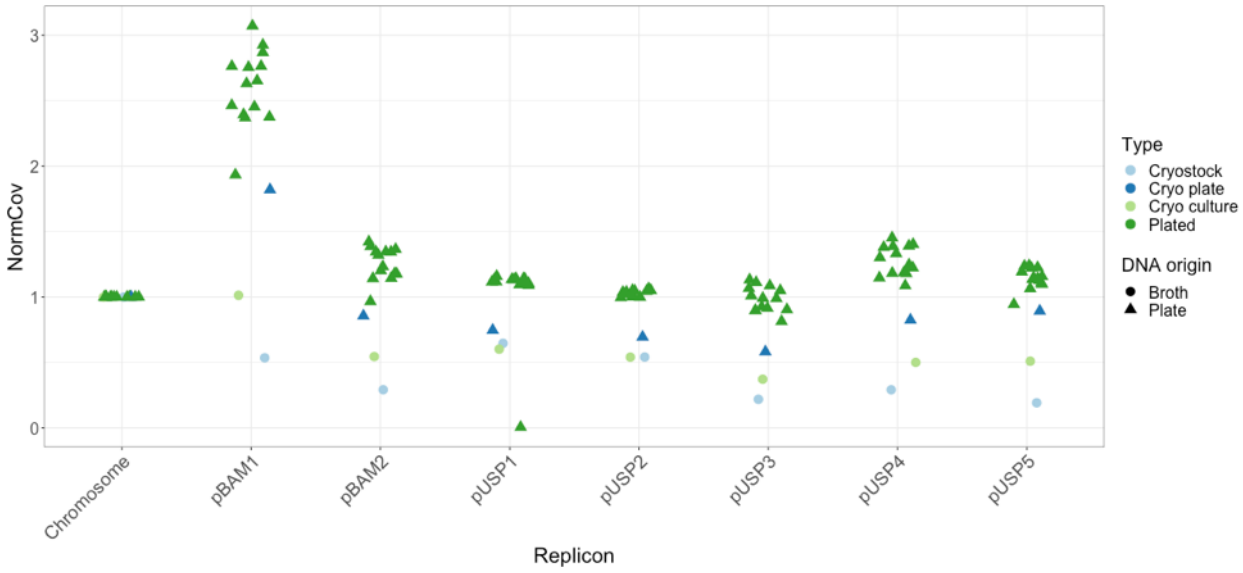


**Figure 5.** Coverage of replicons normalized to chromosome coverage (NormCov). A NormCov of 1 indicates a single copy per chromosome of a replicon. A NormCov above 1 indicates that there are more copies of a given plasmid than the chromosome per cell. Points have been slightly jittered horizontally to improve visualization of overlaps.

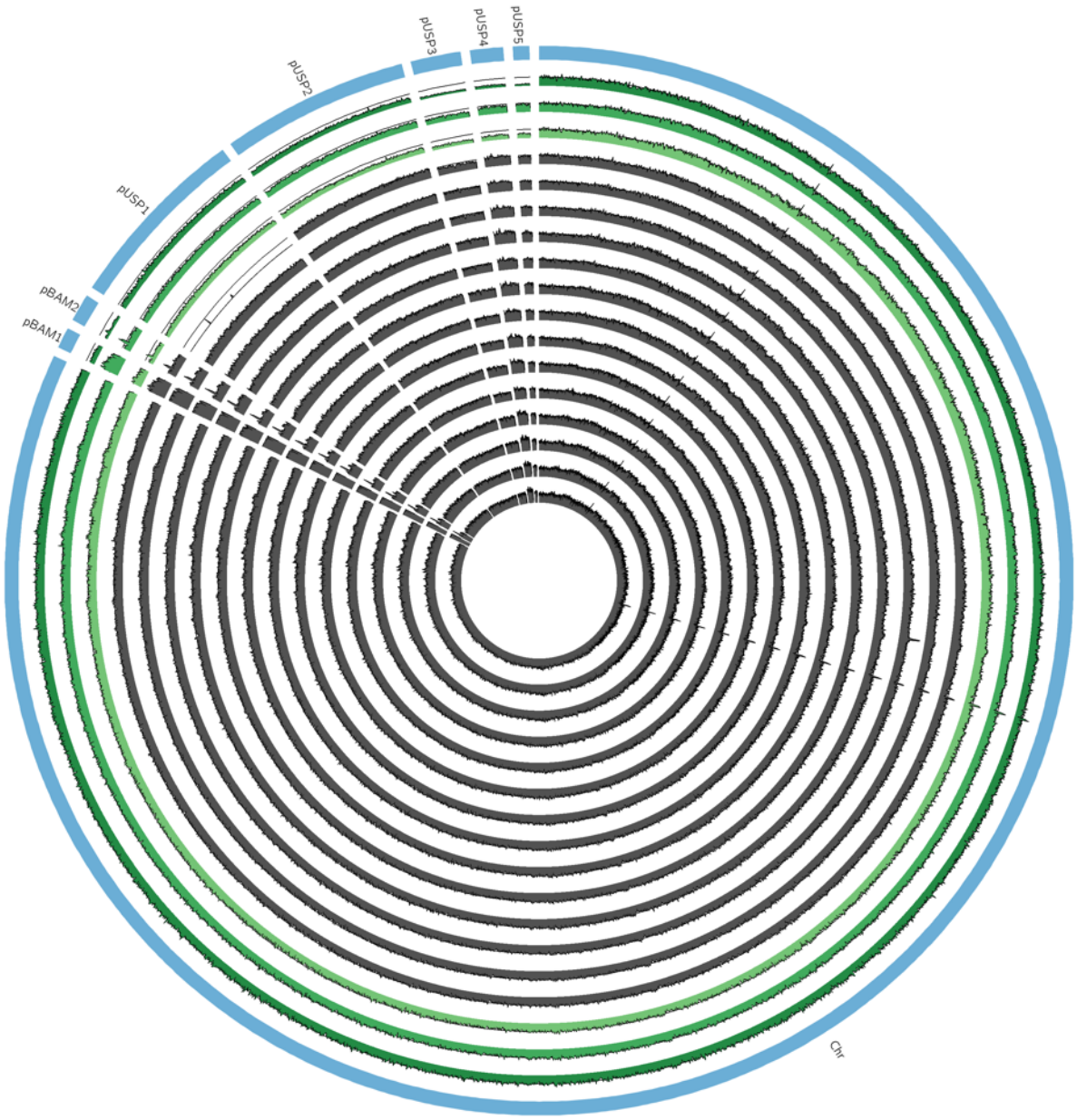


**Figure 6.** Illumina reads mapped to the chromosome and plasmids of MSH1 (DK1 substrain). The outer blue ring indicates the replicons. The inner rings show read mapping coverage of the replicons, normalized to the coverage of the chromosome per replicate, for all of the 17 sequenced replicates. The three first green rings show replicates cryostock, first colony from R2A plate, first colony from R2B broth, respectively. The subsequent 14 grey rings show the replicates that all originate from the same first colony. A solid line in the background of all tracks indicate the

668 chromosome coverage line. Coverage above this line indicates a replicon copy number higher than

669 1 per chromosome and vice versa.

# Supplementary data

**Supplementary Table S1**. Digital DNA:DNA hybridization (dDDH) results from the online Type Strain Genome Server (TYGS) analysis. d0, d4, d6 refers to different algorithms used TYGS. Formula d0 (a.k.a. GGDC formula 1): length of all HSPs divided by total genome length. Formula d4 (a.k.a. GGDC formula 2): sum of all identities found in HSPs divided by overall HSP length. Formula d6 (a.k.a. GGDC formula 3): sum of all identities found in HSPs divided by total genome length. C.I.: Confidence interval.

| | | Type Strain Genome Server | | | | | | |
|---|---|---|---|---|---|---|---|---|
| **Query strain** | **Subject strain** | **dDDH (d0, in %)** | **C.I. (d0, in %)** | **dDDH (d4, in %)** | **C.I. (d4, in %)** | **dDDH (d6, in %)** | **C.I. (d6, in %)** | **G+C content difference (in %)** |
| **MSH1** | *Aminobacter niigataensis DSM 7050* | 69.7 | [65.8 - 73.3] | 82.5 | [79.7 - 85.0] | 74.3 | [70.8 - 77.5] | 0.51 |
| **MSH1** | *Aminobacter aganoensis DSM 7051* | 53.4 | [49.9 - 56.9] | 40.2 | [37.7 - 42.7] | 50.5 | [47.5 - 53.6] | 1.01 |
| **MSH1** | *Aminobacter lissarensis DSM 17454* | 40.6 | [37.2 - 44.0] | 30.8 | [28.4 - 33.3] | 37.4 | [34.5 - 40.5] | 0.19 |
| **MSH1** | *Aminobacter aminovorans DSM 7048* | 41.3 | [37.9 - 44.8] | 30 | [27.6 - 32.5] | 37.7 | [34.8 - 40.8] | 0.31 |
| **MSH1** | *Aminobacter ciceronei DSM 15910* | 39.2 | [35.8 - 42.6] | 29.8 | [27.4 - 32.3] | 36 | [33.1 - 39.1] | 0.18 |

| | | | | | | | | |
|---|---|---|---|---|---|---|---|---|
| **MSH1** | *Aminobacter ciceronei DSM 17455* | 39.2 | [35.8 - 42.6] | 29.8 | [27.4 - 32.3] | 36 | [33.1 - 39.1] | 0.18 |
| **MSH1** | *Chelatobacter heintzii DSM 10368* | 38.7 | [35.3 - 42.2] | 29.7 | [27.3 - 32.2] | 35.7 | [32.7 - 38.7] | 0.26 |
| **MSH1** | *Mesorhizobium plurifarium ORS 1032* | 18.9 | [15.8 - 22.5] | 21.9 | [19.6 - 24.3] | 18.5 | [15.9 - 21.5] | 1.19 |
| **MSH1** | *Mesorhizobium waimense ICMP 19557* | 19.1 | [16.0 - 22.7] | 21.7 | [19.5 - 24.2] | 18.7 | [16.0 - 21.7] | 0.49 |
| **MSH1** | *Mesorhizobium australicum WSM2073* | 19.2 | [16.1 - 22.8] | 21.7 | [19.4 - 24.1] | 18.8 | [16.1 - 21.8] | 0.05 |
| **MSH1** | *Mesorhizobium qingshengii CGMCC 1.12097* | 19.5 | [16.3 - 23.1] | 21.6 | [19.3 - 24.0] | 19 | [16.3 - 22.0] | 0.24 |
| **MSH1** | *Mesorhizobium sangaii DSM 100039* | 19.5 | [16.3 - 23.1] | 21.6 | [19.4 - 24.1] | 18.9 | [16.3 - 22.0] | 0.51 |

677